Indonesian Journal of Electrical Engineering and Informatics (IJEEI)
Vol. 12, No. 4, December 2024, pp. 883~894
ISSN: 2089-3272, DOI: 10.52549/ijeei.v12i4.5899

Passive Intermodulation Cancellation in 5G Systems Using Artificial Neural Networks

Khaled M Gharaibeh
Telecommunications Engineering Department of Yarmouk University, Jordan

Article Info

Article history:

Received Sep 19, 2024
Revised Nov 7, 2024
Accepted Nov 21, 2024

Keywords:

Intermodulation Distortion
Passive Intermodulation
Feedforward Neural Networks
PIM Cancellation
5G

ABSTRACT

Passive intermodulation (PIM) has been a serious challenge in 5G Frequency Division Duplexing (FDD) carrier aggregated (CA) wireless systems leading to the degradation of system performance. Digital cancellation techniques have been used to dynamically cancel the time-varying PIM resulting from passive nonlinearities. These techniques are usually based on Volterra-like behavioral models which are very complex and hard to implement. In this paper, a Feedforward Neural Network (FFNN)-based PIM cancellation scheme is proposed for PIM cancellation in a CA FDD wireless system. Simulation of the proposed scheme shows that the FFNN cancellation scheme is capable of acheving above 20-dB PIM cancellation ratio over a 30-dB input power range.

Corresponding Author:

Khaled M Gharaibeh,
Telecommunications Engineering Department
Yarmouk University,
Irbid, Jordan
Email: kmgharai@yu.edu.jo

1. INTRODUCTION

Passive Intermodulation (PIM) is a major challenge in wireless systems that use FDD Carrier Aggregation (CA) such as 5G-New Radio (NR) systems. CA is based on using contiguous or non-contiguous multi component carrier (CC) bands with the objective of increasing system capacity. The problem with transmitted aggregated carriers is that their interaction by a passive nonlinearity leads to the presence of passive intermodulation (PIM) products in the receive band which leak to the receiver via the duplexing stage. These PIM products result in severe interference which renders CA-FDD systems unable to provide the intended capacity by 5G systems [1]. For example, the technical specifications of the 3rd Generation Partnership Project (3GPP) for Release 12 cellular system show that Base Station (BS) radio systems can undergo severe performance degradation as a result of PIM in several FDD band combinations [2].

There are several scenarios where PIM components result in degradation of system performance. For example, in 5G NR systems, spectral regrowth resulting from passive nonlinearities in the receive chain of the Down Link (DL) of the n 25 band interferes with both Uplink (UL) n 25 and the UL n 66 bands. Another scenario is the interference caused by PIM of the two DL signals of the n 25 and n 66 bands as shown in Figure 1 which results in intermodulation products in the UL n 66 and n 25 bands [2]. This interference leads to significant performance degradations such as high noise floor, reduced cell coverage, receiver desensitization or even blocked transmission.

Several approaches have been proposed for overcoming external PIM in CA-FDD systems [2]. Among these, digital cancellation techniques PIM have proved to be most effective as they can dynamically model and cancel the time-varying PIM [2], [4]-[10]. In digital cancellation, a nonlinear behavioral model is constructed to characterize the passive nonlinearity. This model is then used to produce a canceling signal that removes the PIM components at the receiver using adaptive structures. A detailed survey of various digital cancellation schemes that existed in the literature were presented in [1]-[3].

Behavioral models of passive nonlinearities are usually based on either the Volterra model or memory polynomials (MP's) which can account for memory in the PIM generation process as well as the different mutual delays of the transmit signals before PIM generation [4]-[11]. However, Volterra-based models are usually complex as the number of estimated parameters grows rapidly with the maximum considered nonlinearity order. Furthermore, the set of static parameters has to be extracted for each input configuration (input power, frequency range and step, etc.) [6].

Inspired by the advancements of artificial intelligence (AI) in the communication domain, numerous Artificial Neural Network (ANN)-based models have been investigated in the literature for behavioral modeling of nonlinearities in wireless systems [12]-[16]. The ANN based models have been shown to be more flexible than polynomial based methods such as Generalized Memory Polynomials (GMP) which require fitting a large number of coefficients then pruning the coefficients that have negligible effect based on the knowledge of the mechanisms by which nonlinear distortion is generated [16]. Thus, a GMP requires physical insight into the possible mechanisms that contribute to generation of nonlinear distortion to achieve an acceptable model fidelity.

The ANN based models have been shown to be more flexible than polynomial based methods such as Generalized Memory Polynomials (GMP) which require fitting a large number of coefficients then pruning the coefficients that have negligible effect based on the knowledge of the mechanisms by which nonlinear distortion is generated. Thus, a GMP requires physical insight into the possible mechanisms that contribute to generation of nonlinear distortion to achieve an acceptable model fidelity. ANN-based models, on the other hand, can accommodate the variety of mechanisms by which nonlinear distortion is produced without having to increase the complexity of the model [16].

Although significant research has been conducted on using ANN's for modeling and predistortion of nonlinear PA's as well as self-interreference cancellation in wireless systems, limited research has been done on using them for PIM cancellation as discussed in [2]. Jang *et al*. [13] described a FTDNN for modeling PIM, but its applicability was limited to addressing third order intermodulation products exclusively. In addition, the ANN model was not shown to be effective in canceling PIM products. In [12], the authors presented a PIM cancellation system in satellite communications using RTRLNN algorithm. The system extracts the PIM characteristics during a pilot phase and then the ANN model is used to cancel PIM during the on-time. The proposed system was shown to be effective in PIM interference cancellation in terms of improving the Bit Error Rate (BER) performance of a satellite system. However, the performance analysis lacked clear analysis of PIM power reduction.

In principle, the choice of the type of the ANN to be used in modeling nonlinearities depends on the level of complexity required by the behavioral model. Both RTRLNNs and FTDNNs offer unique capabilities for modeling passive intermodulation distortion. RTRLNNs excel in capturing complex temporal dynamics and long-term dependencies, while FTDNNs are well-suited for modeling time delays and short-term memory effects associated with PIM. This comes at the expense of computational complexity of the ANN as FTDNN's have simpler feedforward connections with time delays than the RNN especially if the time delays are relatively small and the network is not too deep [2].

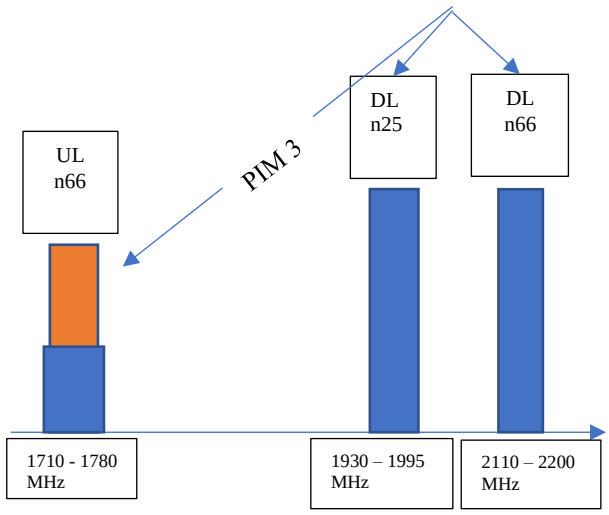

Figure 1. PIM in 5G NR system.

This paper proposes using a FFNN to develop a cancellation scheme for PIM components in a CA-FDD system. The FFNN model is used to predict PIM components when two signals from two frequency bands are

transmitted on the same antenna in an FDD system. The predicted PIM components are then used to cancel the PIM components from the received signal. The contributions of this paper can be summarized by the following:

- The paper presents a novel cancellation scheme for PIM in CA-FDD systems based on prediction of PIM using an FFNN, offering an alternative to the cumbersome Volterra based models.
- The proposed scheme capable of cancelling PIM components of any nonlinear order that lie at intermodulation frequencies and is not limited to third order PIM products, as in the case with most cancellation schemes presented in the literature.
- The proposed model is compared to other approaches presented in the literature and is shown to provide higher PIM cancellation in a 5 G system scenario.

This paper is organized as follows. In Section 2, a detailed description of the mechanism by which PIM is generated and canceled in a CA-FDD receiver is provided. The proposed FFNN model, used to model and cancel the passive nonlinearity, along with its parameter estimation process is then explained. Section 3 presents simulation results, where the FFNN-based PIM cancellation scheme is implemented in MATLAB. Its effectiveness in canceling PIM is assessed and compared to other approaches in the literature. Finally, a concise conclusion of the paper contributions and results is provided in the last section.

2. RESEARCH METHOD

2.1. PIM Generation in CA-FDD Systems

Figure 2 shows PIM generation process in a CA-FDD system. The DL transmitter transmits two CA signals centered at frequencies f_1 and f_2 which produce a PIM component that leak to the receiver through the duplexer. To analyze this scenario, let the transmitted signals be represented as complex discrete signals $x_1(n)$ and $x_2(n)$, then the received baseband UL signal can be expressed as [18]:

$$r(n) = r_0(n) + p(n) + v(n) \tag{1}$$

where $r_0(n)$ represents the uplink signal, $p(n)$ represents the PIM signal generated from the intermodulation of the transmitted signals $x_1(n)$ and $x_2(n)$ which lies in the receive band (at center frequency f_{Rx}), and $v(n)$ is additive white Gaussian noise. For a memoryless passive nonlinearity, the PIM signal $p(n)$ can be expressed as:

$$p(n) = \mathrm{BPF}_{\mathrm{f_{RX}}}\{y(n)\} \tag{2}$$

where $y(n) = F\big(x_1(n), x_2(n)\big)$, the functional $F(\cdot)$ represents the nonlinear characteristics of the passive nonlinearity, and BPF denotes the receive filter centered at f_{RX}. Note that the intermodulation components generated by the term $F\big(x_1(n), x_2(n)\big)$ are located at the intermodulation frequencies $f_{IMD} = |\pm nf_1 \pm mf_2|$, where *n* and *m* are integer coefficients [2]. The absolute values of these coefficients $|n + m|$ are known as the orders of the IMD products. For example, the 3rd order IM (IM3) products, such as $2f_2 - f_1$ and $2f_1 - f_2$. The PIM products of interest are those that lie in the receive band represented by $p(n)$, i.e. $f_{IMD} = f_{RX}$. In principle, the filtered version of the output of the nonlinearity can include any of the intermodulation products that lie in a certain receive band and not be limited to third order PIM products. In the following sections, the PIM cancellation scheme considers all the orders of PIM as these may be present in the UL at higher transmit power levels.

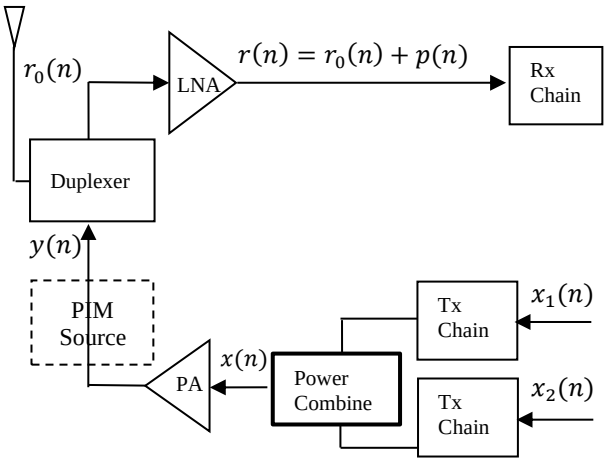

Figure 2. PIM generation in CA-FDD systems.

2.2. Modelling and Cancellation of PIM

A PIM cancellation scheme is depicted in 0. In this scheme, the downlink transmitter transmits two aggregated carriers $x_1(n)$ and $x_2(n)$ which are centered at frequencies f_1 and f_2. The Uplink (UL) signal available at the receiver, consists of the received signal plus PIM components that leak from the transmitter as given in (1). To simplify the analysis, only passive nonlinearities are considered (active nonlinearities of the Low Noise Amplifier (LNA) and the Power Amplifier (PA) are neglected). The PIM estimation block produces a behavioral model for the passive nonlinearity by comparing the transmitted signal to the output of the passive nonlinearity at the receiver during offline operation (training mode). In this mode of operation, the UL received signal (denoted by $r_0(n)$) is absent and hence, the available signal at the receiver consists of only the leaked PIM signal from the transmitter $r(n) = p(n)$ given in (2). The model parameters produced at the training stage and then used to produce a cancelling signal. The cancelling signal is expressed as

$$z_c(n) = H\big(x_1(n), x_2(n)\big) \tag{3}$$

where $H(\cdot)$ represents the behavioral model of the passive nonlinearity represented by the transformation $F(\cdot)$ in (1).

During online operation, the cancelling signal is fed to the receiver to cancel the PIM interreference as shown in 0. In this case, the received signal is

$$r(n) = r_0(n) + p(n) \tag{4}$$

Hence, the signal at the receiver chain is

$$r_c(n) = r(n) - z_c(n) = r_0(n) + v(n) \tag{5}$$

which consists of the received signal with PIM component cancelled.

Note that the above approach for PIM cancellation is based on offline estimation which requires frequent parameter estimation as PIM products may fluctuate in time [17]. This issue can be dealt with through the ANN parameter estimation which will be discussed in the following section.

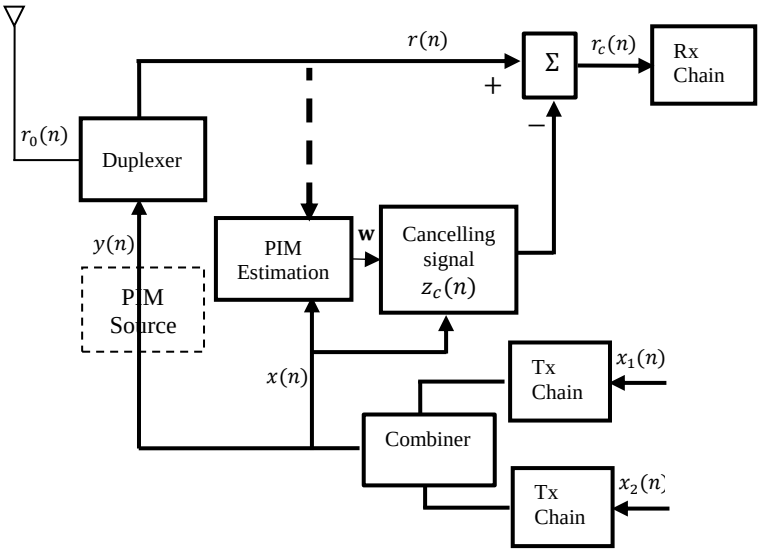

Figure 3. PIM Cancellation scheme in a CA-LTE system.

2.3. Modelling and Cancellation of PIM Using FFNN

The cancellation scheme shown in Figure 3 consists PIM estimation block which is used to produce the canceling signal. The PIM estimation block produces a behavioral model for PIM from the input/output data during a training period as shown in the previous section. In this paper, the behavioral model $H[\cdot]$ in (3) will be developed using an FFNN where a set of weights are estimated from the input/output PIM data and then used by the PIM estimation block to produce the cancelling signal.

The proposed FFNN structure is an ANN, which consists of an input layer, a number of hidden layers and an output layer as shown in Figure 4. In this structure, the structure updates the weights *w* until a minimum error between the output data of the network and the target data is obtained. The output of the hidden layer l is

applied to a nonlinear activation function g_l while the output of the output layer is applied to a linear activation function g_o. The purpose of the activation functions is to provide non-linearity to the neural network; as without the nonlinear activation function, the neural network could only compute linear mappings from inputs to outputs.

The proposed FFNN for PIM signal estimation is based on a 4-input and 2-output structure [14] as shown in 0. The input to the FFNN consists of the in-phase ($I(n)$) and the quadrature components ($Q(n)$) of the complex baseband signals $x_1(n)$ and $x_2(n)$ with center frequencies f_1 and f_2 which can be expressed as:

$$x_1(n) = I_1(n) + jQ_1(n) \quad (6)$$
$$x_2(n) = I_2(n) + jQ_2(n) \quad (7)$$

The input vector $X(n)$ is given by

$$X(n) = [I_1(n), Q_1(n), I_2(n), Q_2(n)] \quad (8)$$

The output of each layer can be expressed by the following equation [13]:

$$a_j^{(1)} = g_1\left(\sum_{i=1}^{q} w_{ji}^{(1)} X_i(n) + b_j^1\right), \quad 1 \le j \le N_{h1} \quad (9)$$

where *j* is the input layer neuron number, w_{ji}^1 is the synaptic weights of the input layer which connect the input *i* to the neuron *j*, N_{h_1} is the number of neurons in the input layer and g_1 is the activation function of the input layer. The output of the *l*-th hidden layer can be written in a similar way to (9) as:

$$a_k^{(l)}(n) = g_l\left(\sum_{j=1}^{N_{h_{l-1}}} w_{kj}^{(l)} a_j^{(l-1)} + b_k^{(l)}\right) \quad (10)$$

where *j* represents the hidden layer neuron number *l*, w_{kj}^l is the synaptic weights connecting the output of the hidden layer $l-1$ to the neuron *j* in layer *l*, $N_{h_{l-1}}$ is the number of neurons in the hidden layer $l-1$ and g_l is the activation function of the layer. The output of the hidden layer in (10) is applied to the next layer, hence, the output of the FFNN is computed using a linear combination of the last hidden layer activations as:

$$I_{out}(n) = g_o\left(\sum_{k=1}^{N_{h_L}} w_{1k}^{(L+1)} a_k^{(L)} + b_1^{(L+1)}\right)$$
$$Q_{out}(n) = g_o\left(\sum_{k=1}^{N_{h_L}} w_{2k}^{(L+1)} a_k^{(L)} + b_1^{(L+1)}\right) \quad (11)$$

where g_o is the output activation function and the output of the model is $p(n) = I_{out}(n) + jQ_{out}(n)$.

The choice of the function g_l depends on the computational efficiency, convergence characteristics of the NN and the values that the input signal take. Therefore, Various activation functions can be used. The most common activation functions as the sigmoid function, hyperbolic tangent sigmoid (tanh), Rectified Linear Unit (ReLU) function, Leaky ReLU, Exponential Linear Unit (ELU), etc. [17]. The choice of the function depends on the computational efficiency, convergence characteristics of the NN and the values that the input signal take.

In this paper, the ReLU activation function is used in the hidden layers as it provides a more effective training process than other functions for the problem in hand. The ReLU activation function is given by [21]:

$$g_l(x) = \begin{cases} \alpha x & x \le 0 \\ x & x > 0 \end{cases} \quad (12)$$

For the output layer, the activation function used is the $purelin$e function which is a linear function that can be expressed as:

$$g_o(x) = purelin(x) = x \quad (13)$$

2.4. Parameter Estimation

The FFNN weights are developed at the training phase using backpropagation-based supervised learning [21]. The network uses batches of training data to minimize a cost function of the form:

$$E = \frac{1}{2N}\sum_{n=1}^{N}\left[\left(I_{out}(n) - \hat{I}_{out}(n)\right)^2 + \left(Q_{out}(n) - \hat{Q}_{out}(n)\right)^2\right] \quad (14)$$

where $I_{out}(n)$, $Q_{out}(n)$ are the IQ components of the true PIM component and $\hat{I}_{out}(n)$ $\hat{Q}_{out}(n)$ are the estimated IQ components of PIM signal by the FFNN. The weights connected to layer l are updated as follows:

$$w_{ji}^l(n+1) = w_{ji}^l(n) + \Delta w_{ji}^l(n) \quad (15)$$

where $w_{ji}^{l}(n)$ is the weight at time n and the adjustment term $\Delta w_{ji}^{l}(n)$ is computed by Adaptive Moment Estimation (ADAM) [16] in which the cost function is iteratively minimized until the preset target performance is achieved. The weights of the FFNN are updated after a batch of samples from the training data set which typically consists of few hundreds of samples. Selecting the size of the batch requires a compromise between the memory size and the speed of convergence [22]. Note that the NN weights are assumed to be estimated during off-line operation. However, this does not mean that the UL transmission needs to be interrupted as the NN can be trained in idle time slots or during lower traffic period.

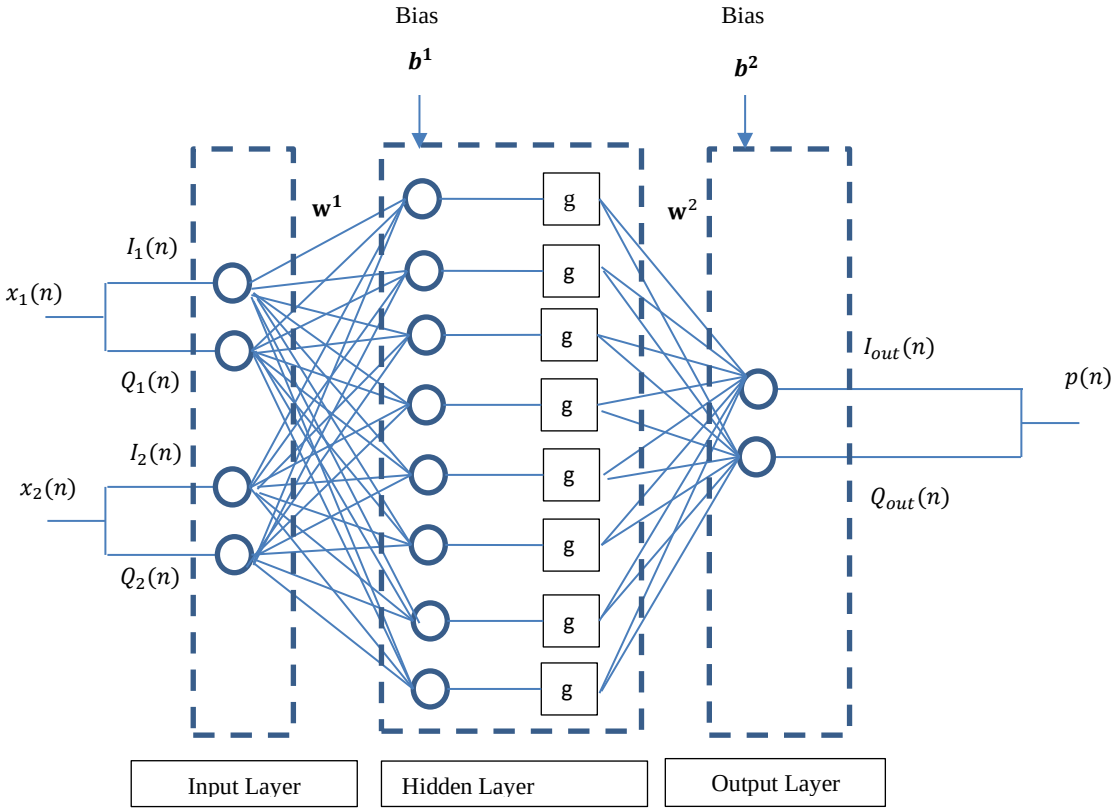

Figure 4. A 4-input-2-output FFNN.

2.5 Limitations of the Proposed Approach

Although the FFNN based canceller provides a simpler way than Volterra and polynomial based cancellers in terms of complexity, the NN model has a number of limitations. On of the main limitations is that the NN model does not have a physical insight into the process by which PIM occurs. Consequently, the NN requires retraining and parameters adjustment when PIM is generated by a different mechanism. The dependence of the model accuracy on the training data is a common challenge with NN models in many applications and specifically in wireless system applications. There are numerous approaches to address this issue in order to enhance the training diversity and reduce potential bias in model performance. These approaches include using incremental learning, pre-training through synthetic data generation or transfer learning [22]-[24].

Another common limitation of the NN model is its high computational complexity necessitating significant computational resources to perform the modeling task in the PIM cancellation scheme. Fortunately, most 5-6G systems are increasingly providing high computational capability through GPUs and AI processers which can facilitate the deployment of ANN-based solutions in real-time applications, including PIM cancellation [25],[27].

3. RESULTS AND DISCUSSION

The objective of the simulations that will follow is to verify the proposed NN-based PIM cancelation scheme in 0 through processing CA-OFDM signals that represent 5G signals. The input to the system (transmit signals) consists of two OFDM carriers of 20 MHz bandwidth with a 120 MHz carrier separation. All signals were generated in Matlab and the FFNN cancellation scheme was implemented using the Deep Learning Toolbox in Matlab.

3.1 PIM Signal Generation

The input OFDM signals were generated according to the specifications shown in Table 1. The training set of the NN was generated using a nonlinear transformation of the two CA OFDM signals mentioned above which represent 5G signals by a nonlinear transformation that represent a passive nonlinearity (PIM source).

The passive nonlinearity was generated using the "Saleh" model which consists of amplitude and phase transformation [28]. For an input signal of the form $x(t) = A(t)e^{j\Phi(t)}$, where $A(t)$ is the signal magnitude and $\Phi(t)$ is its phase, the output of the model is given by [28]-[29]:

$$y(t) = \frac{u_1 A(t)}{(1+v_1 A(t)^2)} \quad e^{\left(\Phi(t)+\frac{u_2 A^2(t)}{(1+v_2 A^2(t))}\right)} \tag{16}$$

where u_1, v_1, u_2 and v_2 are the model parameters which can be estimated from measurements of input/output characteristics of the PIM source [28]. The model parameters were selected as $u_1 = 0.95$; $v_1 = 0.0000095$; $u_2 = 0.5$ and $v_2 = 0.1$.

Note that the PIM source is used for the purpose of verifying the concepts and ensure that the proposed FFNN-based cancellation scheme provides PIM cancellation. In principle, the FFNN can be trained for any random real PIM source or communication signals and is not restricted to a cerain type of passive nonlinearity.

Table 1. Simulation parameters of OFDM signals

Signal length	200000 samples
No. of sub-carriers	2048
Subcarrier spacing	15 kHz
Modulation	16 QAM
Bandwidth	20 MHz
Pulse shaping	Raised Cosine *r*=0.22
Oversampling factor	64
PAPR	10.8 dB
Input power range	10 dBm to 40 dBm

3.2 PIM Cancellation Results

The PIM estimation block consists of a NN which produces a behavioral model for the passive nonlinearity at the training stage and then, the NN weights are used to produce the cancelling signal during a testing phase. In the training phase, the NN model compares a filtered version of the output of the nonlinearity which consists of the PIM components only with the input CA signals $x_1(t)$ and $x_2(t)$ to produce the NN weights using Adaptive Moment Estimation (ADAM). The NN weights *w* are then used to produce the cancelling signal $z_c(n)$ in (3).

The modeling process was conducted using two CA-OFDM signals generated using the specifications in Table 1. Each signal has a length of 200,000 samples of which 70% of the samples are used for model training, while the remaining 30% constitute a test set to evaluate the performance and generalization capability of the model.

The FFNN architecture consists of an input layer, followed by three hidden layers with 128 neurons each, and a dense output layer. The input and hidden layers use the ReLU activation function, while the output layer employs a linear activation function. The network is trained using the ADAM optimizer, an initial learning rate of 0.01 and a batch size of 65000 samples. The training process spans 200 epochs, and its performance is monitored by observing the evolution of the MSE defined in (14) with the iteration number.

Fig. 5 shows the MSE wersus iteration number for the training process of the FFNN, used to model the 3rd order PIM component at transmit power of 30 dBm. The results indicate that the FFNN model converges after approximately 400 iteration. Notable, the number of iterations required for convergence depends on the transmit power level and the PIM order of interest.

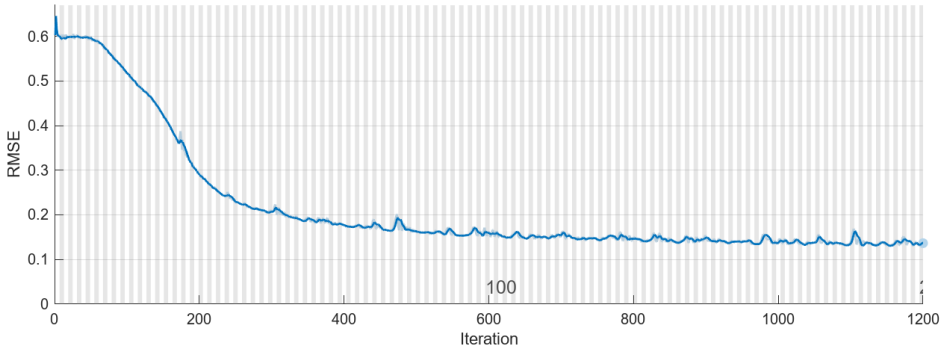

Figure 5. MSE vs transmit power for various PIM orders.

To assess the performance of the proposed PIM cancellation scheme shown in Fig. 3, the PIM component leaking to the receiver was obtained by applying a bandpass filter to the output of the PIM source, $y(n)$. The filtered PIM component was then fed to the cancellation scheme which utlilizes the FFNN to produce a cancelling signal. The cancelling signal was then subtracted from the output the of the PIM source to produce a signal with a cancelled PIM component, denoted as $y_c(n)$ in the following discussion.

The cancelation capability of the proposed scheme are assessed by comparing the power spectral density (PSD) of the output of the passive nonlinearity before and after cancellation of the PIM component of interest. The PSD was computed using a periodogram as [30]:

$$\boldsymbol{S_{yy}(\omega) = \frac{1}{M}|\mathbf{DTFT}(y_w(n)|^2|} \boldsymbol{= \frac{1}{M}\left|\sum_{n=0}^{M-1} y_w(n)e^{-j\omega n}\right|^2} \quad (17)$$

where DTFT denotes the Discrete Time Fourier Transform, $y_w(n) = y(n)W(n)$ is the windowed signal, $W(n)$ is the window function and M is the signal size. The simulations use a Hanning window which, as shown in [30], provides better performance in PIM simulation compared to other window functions.

Figures 6(a)-(d) show the PSD of the input of the cancellation loop (output of the passive nonlinearity before cancellation) and the output of the cancellation loop for the two-carrier aggregated OFDM signals at a transmit power of 30 dBm. The figures show that the power of the PIM component of interest is significantly reduced. The PIM components where cancelled individually in order to evaluate the effectiveness of the cancellation scheme. The results show that the proposed method achieves excellent cancellation of the PIM component of interest, with the resulting cancelled signal approaching the noise floor.

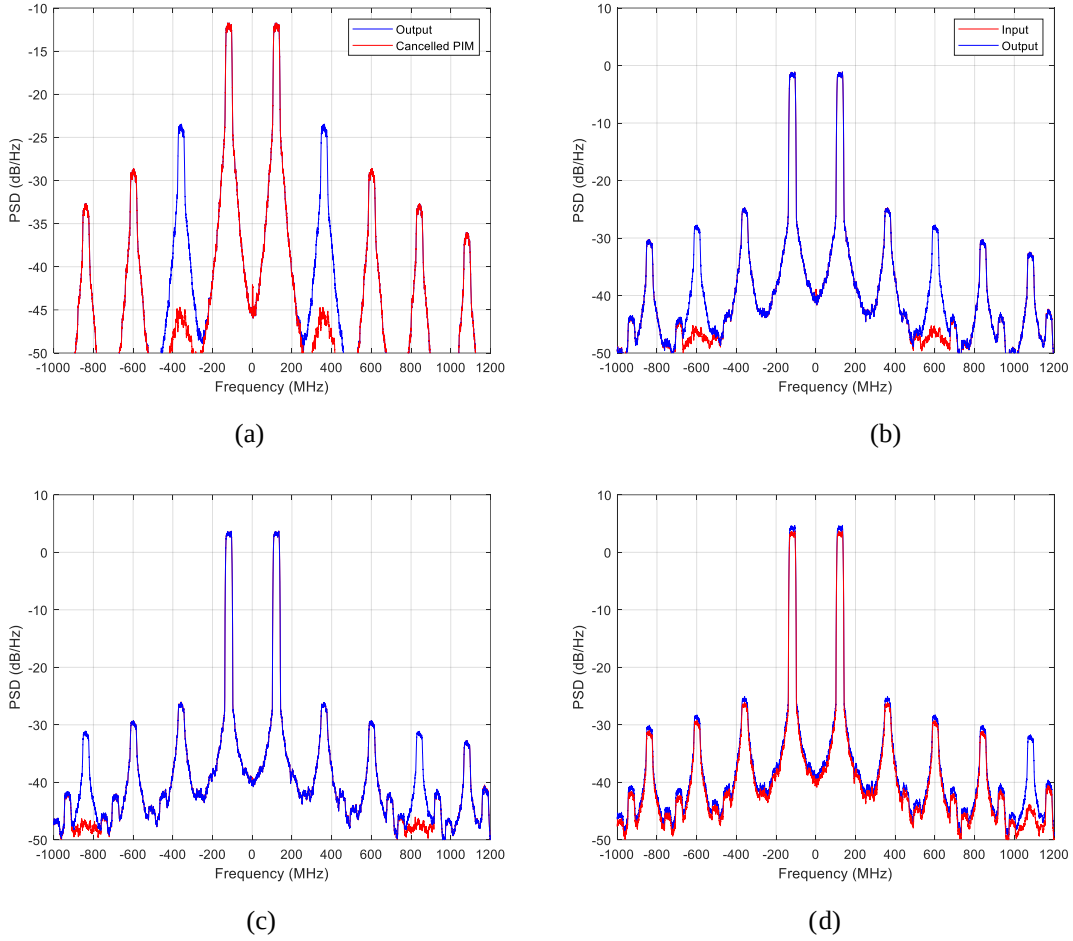

Figure 6. PSD of the input and output of the cancellation scheme dBm; (a): PIM3, (b): PIM5, (c): PIM7 and (d): PIM9.

The PIM cancellation ratio is quantified as:

$$C_k = 10\log_{10}\frac{\int_{\omega_{IM_k}-B_k}^{\omega_{IM_k}+B_k} S_{yy}(\omega)d\omega}{\int_{\omega_{IM_k}+B_k}^{\omega_{IM_k}-B_k} S_{y_cy_c}(\omega)d\omega} \quad (17)$$

where k indicates the k-th PIM compoenent, B_k is the bandwidth of the k-th PIM compoenent, $S_{yy}(\omega)$ is the PSD of the output of the PIM source $y(n)$ defined in (2) and $S_{y_c y_c}(\omega)$ is the PSD of the output of the PIM source after cancelling the k-th order PIM component $y_c(n)$.

Figure 7 shows the PIM cancellation ratio versus transmit power for third, fifth, seventh and ninth PIM components within a transmit power range of 30 dBm. The figure demonstrates that the FFNN based PIM cancellation scheme achieves up to 22 dB cancellation for the third order PIM while the cancellation ratio decreases for higher PIM orders. The reason for this is that higher order PIM components have lower power resulting in reduced cancellation ratio.

Additionally, the figure shows that the cancellation ratio decreases as the the transmit power decreases. This is a direct result of compression in the nonlinear characterteristic of the Saleh model, which becomes more pronounced at higher at high input power levels. Operating the PIM source closer to the compression point of its nonlinear characteristic reduces the model accuracy which is a typical phenomenon observed in most nonlinear modelling approaches.

However, with NN models, the range of transmit power where the model provides acceptable PIM cancellation can be expanded by enhancing the training data set. Specifcally, including more samples that drive the PIM source near its compression point allows the FFNN to learn the complex nonlinear behavior more effectively, improving its cancellation performance in challenging condition.

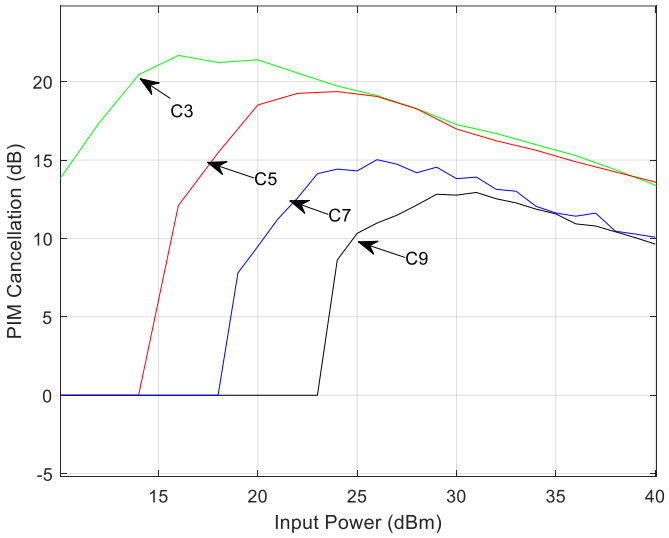

Figure 7. PIM cancellation versus transmit power.

The Signal to Interference Ratio (SIR) is also used to quantify the cancellation performance of the model. The SIR before PIM cancellation is given by

$$SIR = 10\log_{10}\frac{\int_{-B_0}^{+B_0} S_{rr}(\omega)d\omega}{\int_{\omega_{IM_k}-B_k}^{\omega_{IM_k}+B_k} S_{yy}(\omega)d\omega} \quad (18)$$

where $S_{rr}(\omega)$ is the PSD of the received signal, B_0 is the receive signal bandwidth and B_k is the bandwidth of the PIM component of interest. The SIR after cancellation is expressed as:

$$SIR = 10\log_{10}\frac{\int_{-B_0}^{+B_0} S_{rr}(\omega)d\omega}{\int_{\omega_{IM_k}-B_k}^{\omega_{IM_k}+B_k} S_{y_c y_c}(\omega)d\omega} \quad (18)$$

Fig. 8 shows the SIR versus the transmit power before and after cancellation of the 3rd order PIM component assuming a receiver signal power of 30 dBm. The figure demonstrates that the PIM cancellation scheme achieves an SIR gain of 15-25 dB, highlighting that the porposed cancellation scheme provide significant performance improvement in CA-FDD wireless systmes.

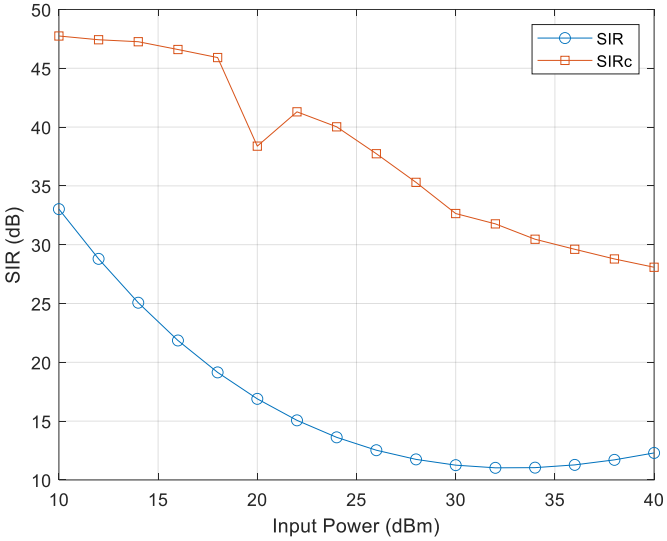

The PIM cancellation results presented in this paper were compared to those reported in the literature. Table II summarizes the PIM cancellation performance of various Volterra-based cancellation approaches. The results demonstrate that the proposed FFNN-based cancellation approach achieves significantly higher cancellation of PIM components compared to other methods. This superior performance can be attributed to the fact that NN models are universal approximators where they can model complex and high order nonlinearities without being explicitly tied to a predefined mathematical structure as Volterra based models. Additionally, while some methods in the literature achieve comparable results under specific conditions, the proposed approach maintains consistent performance across a wider range of input power levels and PIM orders, as shown in Fig. 7.

Table 2. Comparsion of the proposed approach to literature

Reference	Approach	PIM Cancellation C_k
[1], [4] Lampu et. al	Generalized Memory Polynomial (GMP)	15-18 dB
[5], [6] Tian, et. al	Hammerstein Model	10 dB gain in SIR
[12] Liang et. al	RTLNN	10 dB gain in SIR
[7] Liu et. al	Wiener-Hammerstein model / B-spline	19 dB
[7] [10]Waheed, et al	Generalized Memory Polynomial (GMP)	19 dB
[17] Ahmed et. al	Generalized Memory Polynomial (GMP)	12-14 dB
The proposed approach		22 dB

4. CONCLUSION

A FFNN-based cancellation scheme for mitigating PIM in CA-FDD systems has been presented and verified. The proposed scheme utilizes an FFNN to model passive nonlinearity that exist at the duplexing stage. The FFNN model is trained offline, during which the network weights are produced and stored. These weights are subsequently used during online operation to generate a cancelling signal for PIM mitigation.

Simulation results demonstrate that the proposed scheme achieves over 22 dB of cancellation for 3rd order PIM components when two CA-OFDM signals emulating 5G signals are applied. The proposed FFNN-based cancellation scheme has been compared to Volterra based cancellation schemes and has been shown to achieve better PIM cancellation. Moreover, the proposed scheme is not limited to cancelling 3rd order PIM products alone; it is capable of effectively cancel PIM components of any order.

REFERENCES

[1] V. Lampu, L. Anttila, M. Turunen, M. Fleischer, J. Hellmann, and M. Valkama, "Air-induced Passive Intermodulation in FDD MIMO Systems: Algorithms and Measurements," *IEEE Trans. Microwave Theory Techn*., vol. 71, no. 1, pp. 373-388, 2022.

[2] T. Ahmmed, A. Kiayani, R. M. Shubair, and H. Yanikomeroglu, "Overview of Passive Intermodulation in Modern Wireless Networks: Concepts and Cancellation Techniques," *IEEE Access*, vol. 11, pp. 128337-128353, 2023.

[3] H. M. Karaca, “Passive Inter-modulation Sources and Cancellation Methods,” *Eur. J. Res. Dev.*, vol. 2, no. 2, pp. 75-91, 2022.
[4] V. Lampu, L. Anttila, M. Turunen, M. Fleischer, J. Hellmann, and M. Valkama, “Air-induced PIM Cancellation in FDD MIMO Transceivers,” *IEEE Microw. Wireless Compon. Lett.*, vol. 32, pp. 780–783, Jun. 2022.
[5] L. Tian, H. Han, W. Cao, X. Bu, and S. Wang, “Adaptive Suppression of Passive Intermodulation in Digital Satellite Transceivers,” *Chin. J. Aeronaut.*, vol. 30, pp. 1154–1160, Jun. 2017.
[6] X. Miao and L. Tian, “Digital Cancellation Scheme and Hardware Implementation for High-order Passive Intermodulation Interference Based on Hammerstein Model,” *China Commun*., vol. 16, no. 9, pp. 165–176, 2019.
[7] M. Z. Waheed et al., “Passive Intermodulation in Simultaneous Transmit–Receive Systems: Modeling and Digital Cancellation Methods,” *IEEE Trans. Microwave Theory Tech.*, vol. 68, no. 9, pp. 3633–3652, Sep. 2020.
[8] J. Liu, X. Zhang, J. Yang, and H. Yang, "Digital Cancellation of Multi-band Passive Inter-modulation Based on Wiener-Hammerstein model," *Digital Commun. Netw*., vol. 10, no. 4, pp. 1189–1197, Aug. 2024.
[9] K. M. Gharaibeh, “Digital Cancellation of Passive Intermodulation Distortion in Wideband FDD Systems,” *Int. J. Electr. Eng*., vol. 29, no. 6, pp. 179–186, 2022.
[10] M. Z. Waheed et al., “Digital Cancellation of Passive Intermodulation in FDD Transceivers,” in *Proc. 52nd Asilomar Conf. Signals, Systems, Comput*., 2018, pp. 1375–1381.
[11] F. Kearney and S. Chen, “Passive Intermodulation (PIM) Effects in Base Stations: Understanding the Challenges and Solutions*,” Analog Dialogue*, Tech. Rep. 51-03, Mar. 2017.
[12] B. Liang, X. Bu, M. Li, P. Guo, and C. Liu, “A Novel RTRLNN Model for Passive Intermodulation Cancellation in Satellite Communications,” in *Proc. 14th Int. Wireless Commun. Mobile Comput. Conf.* (*IWCMC*), 2018, pp. 18–23.
[13] B. Jang, S. Im, C. Kim, and S. Hong, “Modeling of Passive Intermodulation Distortion Using the Neural Networks and the Cubic Volterra Filter,” in *Proc. Int. Conf. Inf. Commun. Technol. Converg.* (*ICTC*), Oct. 2019, pp. 1042–1046.
[14] B. Jang et al., “PIMD Signal Modeling Based on FTDNN,” in *Proc. IEEE Int. Conf. Inf. Commun. Signal Process.* (ICICSP), Sep. 2019, pp. 1–4.
[15] H. Guo, S. Wu, H. Wang, and M. Daneshmand, “DSIC: Deep Learning Based Self-Interference Cancellation for In-band Full Duplex Wireless,” in *Proc. IEEE Global Commun. Conf.* (*GLOBECOM*), Dec. 2019, pp. 1–6.
[16] F. Diffner, "Explaining Neural Networks Used for PIM Cancellation," M.S. thesis, School of Electrical Engineering and Computer Science, KTH Royal Institute of Technology, Stockholm, Sweden, Sep. 2022.
[17] C. Tarver, L. Jiang, A. Sefidi, and J. R. Cavallaro, “Neural Network DPD via Backpropagation Through a Neural Network Model of the PA,” in *Proc. 53rd Asilomar Conf. Signals, Systems, Comput*., Nov. 2019, pp. 358–362.
[18] T. Ahmmed, Passive Intermodulation Effects in Modern Radio Communication Systems, Ph.D. dissertation, Carleton Univ., Ottawa, ON, Canada, 2024.
[19] X. Hu et al., “Convolutional Neural Network for Behavioral Modeling and Predistortion of Wideband Power Amplifiers,” *IEEE Trans. Neural Netw. Learn. Syst.*, vol. 33, no. 8, pp. 3923-3937, 2021.
[20] O. Yildirim, “Passive Inter-modulation Sources and Cancellation Methods,” *Sensors Transducers*, vol. 256, no. 2, pp. 36-44, 2022.
[21] X. Hu et al., “Convolutional Neural Network for Behavioral Modeling and Predistortion of Wideband Power Amplifiers,” *IEEE Trans. Neural Netw. Learn. Syst.*, vol. 33, no. 8, pp. 3923-3937, 2021.
[22] M. Z. Alom, T. M. Taha, C. Yakopcic, S. Westberg, P. Sidike, M. S. Nasrin, B. C. Van Esesn, A. A. S. Awwal, and V. K. Asari, "The History Began from AlexNet: A Comprehensive Survey on Deep Learning Approaches," *arXiv preprint arXiv:1803.01164*, 2018.
[23] M. Chen, U. Challita, W. Saad, C. Yin, and M. Debbah, "Machine Learning for Wireless Networks with Artificial Intelligence: A Tutorial on Neural Networks," *arXiv preprint arXiv:1710.02913*, Oct. 2017.
[24] S. S. Sarwar, A. Ankit, and K. Roy, "Incremental Learning in Deep Convolutional Neural Networks Using Partial Network Sharing," *IEEE Access*, vol. 8, pp. 4615-4628, 2019.
[25] M. M. Hasan, “Implementation of Neural Network Adaptive Digital Pre-distortion for Wireless Transmitters,” Ph.D. dissertation, Univ. Calgary, Calgary, Canada, 2015.
[26] M. Shao, J. Zhang, J. Lin, and Z. He, "5G and Beyond: GPU and FPGA Accelerated Parallel Computing Architectures for Deep Learning," *IEEE Wireless Commun*., vol. 28, no. 1, pp. 54–61, Feb. 2021.
[27] Z. Liu, Y. Huang, and J. Zhang, "AI-Driven Real-Time Interference Mitigation in 5G Networks using FPGA-based Neural Network Accelerator," in *Proc. IEEE Globecom Workshops (GC Wkshps)*, Dec. 2020, pp. 1–6.
[28] M. O'droma, S. Meza, and Y. Lei, “New Modified Saleh Models for Memoryless Nonlinear Power Amplifier Behavioural Modelling,” *IEEE Commun. Lett*., vol. 13, no. 6, pp. 399-401, 2009.
[29] J. Sombrin, G. Soubercaze-Pun, and I. Albert, “New Models for Passive Nonlinearities Generating Intermodulation Products with Non-integer Slopes,” in *Proc. Eur. Conf. Antennas Propag.* (EuCAP), Apr. 2013, pp. 25–28.
[30] K. M. Gharaibeh, “Assessment of Various Window Functions in Spectral Identification of Passive Intermodulation,” *Electronics*, vol. 10, no. 9, p. 1034, Apr. 2021.

[31] S. Zhang, X. Hu, Z. Liu, L. Sun, K. Han, W. Wang, and F. M. Ghannouchi, "Deep Neural Network Behavioral Modeling Based on Transfer Learning for Broadband Wireless Power Amplifier," *IEEE Microw. Wireless Compon. Lett*., vol. 31, no. 7, pp. 917-920, Jul. 2021.

BIOGRAPHY OF AUTHORS

Khaled M Gharaibeh received his B.S. and M.S. in Electrical Engineering in 1995 and 1998 respectively, both from Jordan University of Science and Technology, Irbid, Jordan and his PhD in Electrical Engineering in 2004 from North Carolina State University, Raleigh, NC. He is a Senior member of the Institute of Electrical and Electronics Engineering (IEEE), Microwave Theory and Techniques Society (MTTS), Jordan Engineers Association and the honor society Eta Kappa Nu. His research interests are nonlinear system identification, behavioral modeling of nonlinear RF circuits, Passive intermodulation Cancellation and wireless communications.